HHS Public Access

Author manuscript

J Int Soc Respir Prot. Author manuscript; available in PMC 2023 May 18.

Published in final edited form as:

J Int Soc Respir Prot. 2019 December ; 36(2): 66–76.

Numerical Simulations of Exhaled Particles from Wearers of Powered Air Purifying Respirators

Susan S. Xu,

Zhipeng Lei*,

Ziqing Zhuang,

Michael Bergman

National Institute for Occupational Safety and Health, National Personal Protective Technology Laboratory, Pittsburgh, Pennsylvania 15236

Abstract

In surgical settings, infectious particulate wound contamination is a recognized cause of post-operative infections. Powered air purifying respirators (PAPRs) are worn by healthcare workers for personal protection against contaminated aerosols. Healthcare infection preventionists have expressed concern about the possibility that infectious particles expelled from PAPR exhalation channels could lead to healthcare-associated disease, especially in operative settings where sterile procedural technique is essential.

This study used computational fluid dynamics (CFD) modeling to simulate and visualize the distribution of particles exhaled by PAPR wearers. Using CFD simulations, the PAPR inside to outside ratio of particle concentrations was estimated. Also, the effects of particle sizes, supplied-air flow rates, and breathing work rates on outward leakage were evaluated.

This simulation study reconstructed a geometrical model of a static median headform wearing a loose-fitting PAPR by capturing a 3D image. We defined a mathematical model for the headform and PAPR system and ran simulations with four particle sizes, three breathing workloads and two supplied-air flow rates (a total 24 configurations; 4×3×2=24) applied on the digital model of the headform and PAPR system. This model accounts for exhaled particles, but not ambient particles. Computed distributions of particles inside and outside the PAPR are displayed.

The outward concentration leakage was low at surgical setting, e.g., it was about 9% for a particle size of 0.1 and 1 μm at light breathing and a 205 L/min supplied-air flow rate. The supplied-air flow rates, particle sizes, and breathing workloads had effects on the outward concentration leakage, as the outward concentration leakage increased as particle size decreased, breathing workload increased, and the supplied-air flow rate decreased. The CFD simulations can help to optimize the supplied-air flow rates. When the loose-fitting PAPR is used, exhaled particles with

*Corresponding author: wrt8@cdc.gov.

Disclaimer

The findings and conclusions in this study are those of the author(s) and do not necessarily represent the official position of the National Institute for Occupational Safety and Health, Centers for Disease Control and Prevention. Mention of a company or product name does not constitute endorsement by NIOSH.

small size (below 1μm), or heavy breathing workloads, may generate a great risk to the sterile field and should be avoided.

Keywords

Exhaled particles; outward leakage; powered air purifying respirators; Computational Fluid Dynamics; simulation; surgical setting; sterile surgical field

INTRODUCTION

Contamination of surgical fields is a widely recognized cause of post-operative infections, and the dispersion of pathogens through the air is known as a cause of healthcare-associated infections (HAIs) [Zhou et al, 2015; Lipp, et al, 2014]. Approximately 722,000 HAIs were identified in U.S. acute care hospitals in 2011, including an estimated 157,500 surgical site infections (SSIs) from inpatient surgery [CDC. Healthcare-associated Infections Data.]. The use of personal protective equipment (PPE) for protecting the healthcare worker (HCW) against hazardous source is an important measure to reduce the chances of aerosol transmission.

In addition to protecting HCW against airborne particles, PPE with the use of plastic face shields can protect HCW against contamination from splashes or other liquids [Skinner, et al. 2001]. Recently, the use of powered, air-purifying respirators (PAPRs) by HCW for self-protection has been increasing [Wizner et al, 2016]. PAPRs used in healthcare typically use a battery-operated blower and one or more high-efficiency particulate air (HEPA) filter(s) to provide the wearer with purified air. PAPRs can be separated into two classes depending on how they're worn: a tight-fitting class that forms a seal with the wearer's skin and a loose-fitting class comprised of hoods or helmets that reduce the wearer's exposure to ambient aerosols. Because loose-fitting PAPR hood designs can fully cover the wearer's head and neck to reduce skin contact with body fluids from an infected person, they are well-suited for use by HCWs during aerosol-generating procedures that sometimes pose a higher risk of exposure than routine healthcare duties.

There are situations that healthcare workers and safety professionals would potentially choose a loose-fitting PAPR (e.g., MaxAir® Systems) but concomitant concerns exist that exhaled/expelled, and potentially infectious particulates may contaminate the surgical site. This topic has been the source of controversy among healthcare professionals working in the operating room (OR) [Sreeramoju et al, 2018]. Compared to other types of respirators (e.g., N95 with no exhalation valve), the exhaled air from a PAPR wearer is not filtered, and therefore is generally expected to contain some aerosolized microorganisms.

These exhaled particles contained in the outward leakage from the PAPR wearer can cause infections in surgical settings, which is an important consideration during surgery where a sterile field needs to be maintained. There is debate about where these particles travel to—a literature review yielded limited published studies and data comparing particle concentration in an OR with and without PAPR use. Thus, it remains unknown whether the exhaled

particles are released from PAPR facepiece with additional work needed. Therefore, further investigation of the factors determining particle trajectory from PAPRs is warranted.

There are four respiratory actions that produce airborne particles or droplets: mouth breathing, nose breathing, coughing/sneezing, and talking. In general, coughing produces the largest droplet concentrations and nose breathing the least [Papineni et al, 1997]. Papineni and Rosenthal [Papineni et al, 1997] found the preponderance of particles is less than 1 μm in size during normal breathing and talking. Droplet transmission is pertinent to larger particles that are expelled and rapidly settle to a surface (e.g., the interior surface of a PAPR hood), usually within one minute of production, and the most significant contamination from droplets therefore will be close to the source [Wurie et al, 2013]. Yan and Grantham [Yan et al, 2018] assessed infectious viruses in the exhalation of symptomatic seasonal influenza cases. The results showed that viral Ribonucleic Acid (RNA) of fine and coarse aerosols was positively associated with body mass index of the individual being monitored and the number of coughs, suggesting that transmission of infectious virus in exhalation may be related to breathing patterns.

The authors are aware of only limited pilot experimental studies to compare the particle concentration in an OR with and without PAPRs being used, due to the expense, time and specialized facilities required. Both studies didn't consider variable workloads and supplied-air flow rates. Kim and Hale [Kim et al, 2017] conducted a pilot study to examine the use of a loose-fitting PAPR in the OR and found no discernible differences in the particulate counts at the surgical table when the PAPR-hood system was turned on or off (ranges: 1700–1850 particles/cm^3). Their conclusion was that the hooded PAPR did not noticeably increase particulate transfer to the surgical field. Grinshpun [Grinshpun, 2016] conducted another pilot study to simulate PAPR wearers in an OR to assess the bacterial contamination of sterile field surfaces. He found that when comparing the respiratory and control groups of agar plate location separately, there was no statistically significant difference in the mean contamination values associated with a specific agar plate location for either of the PAPR or N95 respirators tested. However, taken together and on average, the bacterial contamination of sterile fields by a pair of subjects operating in an OR-simulating facility while wearing either PAPRs or N95 respirators is significantly higher than that obtained in both negative control tests.

Remarkably, there are no well-designed empiric studies assessing the exhalation of viable aerosols from PAPRs. In the absence of empiric data, we used computational fluid dynamics (CFD) to study the flow of particles out of loose-fitting PAPRs. Our previous study, using CFD, constructed digital headform models with the biomechanics of breathing to simulate the protection of loose-fitting PAPRs against particles [Lei et al, 2017]. The CFD PAPR model was based on a loose-fitting PAPR system that had a loose-fitting facepiece. In those CFD simulations, the PAPR supplied-air and the cyclic breathing air vented inside the PAPR. The challenge particles, which were the particles outside of the PAPR breathing zone, were introduced at the loose-fitting area where the PAPR loosely fits the headform. The particle concentration of inhalation air was simulated using Eulerian-Lagrangian particle tracking, in which particles are allowed to move relative to the airflow. In a later study from

our group, the computational results of the CFD PAPR models were validated using actual experimental data [Bergman et al, 2018].

This study addresses the flow of particles out of loose-fitting PAPRs. This study focused on three objectives: (1) Utilize CFD modeling to simulate and visualize the distribution of particles exhaled by the PAPR wearers in the breathing zone; (2) Determine the outward leakage of the exhaled particles, i.e., ratio of exhaled particle concentration outside the PAPR to that inside the PAPR as a function of exhaled particle concentrations and sizes; (3) Evaluate the effect of supplied-air flow rates and work rates on outward leakage to better understand the relationships among flow rate, work rate, and outward leakage.

MATERIALS AND METHODS

PAPR Model

The MaxAir® Systems 78SP-36 cuff system with disposable cuff (Bio-Medical Devices, Inc., Irvine, CA) pictured in Figure 1, a popular loose-fitting PAPR model used in healthcare worker settings, was selected to be simulated for this study [5]. It is a helmet-style PAPR where both the filter and blower motor are contained in the helmet. A digital loose-fitting PAPR was created by scanning the geometries of the components of the MaxAir® model and using additional surface processing techniques (i.e., surface smoothing and noise reduction) to achieve a model suited for CFD.

The digitized PAPR model had supplied-air venting holes that were the same number (10) and size (10 mm diameter) as in the physical PAPR. The MaxAir® PAPR had a supplied-air flow rate 205 L/min, which was tested in our laboratory and was higher than 170 L/min, the minimum current NIOSH certification required airflow rates for loose-fitting PAPRs. This study chose the real supplied-air flowrate of 205 L/min and a low supplied-air flowrate 100 L/min to investigate the effects of the flow rates.

Head model

In the CFD model, the NIOSH medium-size digital headform, representing approximately 50% of the current U.S. workforce [Benson et al, 2010], was used to simulate the wearer of a loose-fitting PAPR. The headform used a cylindrical tube, 2 cm in diameter and 10 cm long, connected to the headform's mouth as a breathing airway through which breathing air passes through the mouth and in and out of the airway during CFD simulations. Three respiratory minute ventilations VE (L/min) and corresponding breathing rates f (breaths/minute) were selected in this study, providing a range of respiration from light work to heavy exertion to simulate health care workers in hospitals, as listed in Table I.

CFD Model of PAPR-headform

We constructed a CFD model of the PAPR-headform to mimic the situation in which a loose-fitting PAPR is donned on a manikin. The digital headform virtually donned the digital PAPR model, generating a volume between the headform and the loose-fitting PAPR, which we refer to as the 'breathing zone' into which both the breathing air and the supplied-air streamed. The breathing zone was divided into 913,653 hexahedral cells using

the tool SnappyHexMesh provided by OpenFOAM software (version 4.0, the OpenFOAM Foundation Ltd, London, United Kingdom).

The surface of the CFD model was split into different boundaries, including the surface wall, supplied-air venting, breathing venting, and loose-fitting area, presented in Figure 2. The surface wall consisted of PAPR and headform surfaces and used a non-slip boundary condition, i.e., the flow velocity at the boundary is held at zero. A velocity inlet boundary condition was modeled using a constant flow through the supplied-air venting into the PAPR breathing zone. The breathing venting also used the velocity inlet boundary condition, but with a sinusoidal flow rate to simulate the cyclic breathing pattern including both inhalation and exhalation. The area where the PAPR loosely fits the headform at the neck had an approximately 10 mm gap of about 80 mm wide and 15 mm long. The pressure outlet boundary condition was defined in the loose-fitting area to simulate the airflow exiting the PAPR to the atmosphere.

CFD simulation

This simulation study innovatively developed a CFD model to run 24 simulations with four particle sizes, three workloads, and two supplied-air flowrates (4×3×2=24) applied on a loose-fitting PAPR donned on a digital headform.

In the CFD solver, we defined the mass continuity and the Navier-Stokes equations to describe the interaction of the breathing airflow and supplied-air flow in the PAPR breathing zone, using the assumption of unsteady incompressible flow. The Eulerian-Lagrangian particle tracking technique was used to track particles in the velocity fields of the CFD model. We assumed that only air drag force influences the particle movement and the particle diffusion can be neglected so that the governing equations for the movement of a spherical particle are as follows:

$$m_p \frac{d\boldsymbol{U}_p}{dt} = \boldsymbol{F}_D \tag{1}$$

$$\frac{\mathrm{d}\mathbf{X}_\mathbf{P}}{\mathrm{dt}} = \boldsymbol{U}_p \tag{2}$$

where m_p is the particle mass, U_p is the particle velocity, F_D is the drag force per unit particle mass, and X_p is the particle position [Tsuda et al, 2013]. F_D is dependent on the particle Reynolds number:

$$\boldsymbol{F}_D = \frac{24\upsilon}{d}\frac{3\rho}{4d\rho_P}\left(1 + 0.15\boldsymbol{Re}_P^{0.687}\right)(\boldsymbol{U} - \boldsymbol{U}_p) \tag{3}$$

where ν is the kinematic viscosity, d is the particle aerodynamic diameter, ρ is the air density, ρ_p is the particle density, U is the air velocity, and Re_p is the particle Reynolds number. Re_p is defined as:

$$Re_p = \frac{d|\boldsymbol{U}-\boldsymbol{U}_p|}{\upsilon}. \quad (4)$$

Because the particles had small size (0.1 to 10 μm), we assumed that when particles touched the surface wall boundary, they deposited on the boundary and did not rebound back to the air [Tsuda et al, 2013].

The pisoFoam solver (in OpenFOAM) with the PISO (Pressure Implicit with Splitting of Operators) algorithm was used to perform the CFD simulation since the solver assumes that the flow is transient and incompressible and has a turbulent effect. Each simulation calculated for the duration of three breathing cycles with 0.001-second time-steps; at each time-step, the pressure field and the velocity field inside the PAPR breathing zone were determined. When the breathing was in the exhalation phase, particles with uniform size and concentration of 100 particles/cm^3, were generated in the exhaled air at the breathing airway. Note that this is a nominal concentration for simulation purposes and not necessarily a realistic concentration. Based on Equations (1–4), particle movements were tracked to calculate the number of particles leaking out of the PAPR through the loose-fitting area.

Since the flow rate and the particle concentration of the exhaled air from the mouth opening were defined, we can compute the total number of exhaled particles from the mouth. After the CFD simulations, we monitored the number of exhaled particles leaking outside the PAPR. Then, in each CFD simulation, we determined the outward particle leakage, i.e., the ratio of exhaled particle number leaking outside the PAPR (unit, number of particles) to the inside the PAPR which exhaled particle number from the mouth (unit, number of particles) are:

$$Outward\ Particle\ Leakage = \frac{exhaled\ particle\ number\ outside\ the\ PAPR}{exhaled\ particle\ number\ inside\ the\ PAPR} \quad (5)$$

After the CFD simulations, we also monitored the volume of the air venting outside the PAPR, so that the exhaled particle concentration leaking outside the PAPR can be estimated. In each CFD simulation we determined the outward concentration leakage, i.e., the ratio of exhaled particle concentration leaking outside the PAPR (unit: number of particles/liter of air) to the exhaled particle concentration inside the PAPR (unit: number of particles/liter of air):

$$Outward\ Concentration\ Leakage = \frac{exhaled\ particle\ concentration\ outside\ the\ PAPR}{exhaled\ particle\ concentration\ inside\ the\ PAPR} \quad (6)$$

Both parameters, the outward particle leakage and the outward concentration leakage, can quantitatively indicate the leakage of exhaled particles. The former only considered the particle number; the latter included the influence of airflow volume and was close to the definition of the fit factor in respirator fit tests.

RESULTS AND DISCUSSION

The particle distribution of a CFD simulation (heavy breathing, supplied-air flow rate 205 L/min, and particle size 1 μm) at different time instances is showed in Figure 3. During the first breathing cycle's exhalation, displayed in the time instances t=0.1, 0.2, and 0.5s, the exhaled particles moved out of the mouth opening and occupied the region close to the front face, and part of the exhaled particles leaked outside of the PAPR through the loose-fitting faceseal. During the first breathing cycle's inhalation, presented in the time instances t=1 and 1.5s, part of the exhaled particles was inhaled into the mouth opening. After the first breathing cycle, shown in the time instance t=2.5s, part of the exhaled particles occupied most of the region inside the PAPR, part of them deposited on the face or PAPR, part of them were inhaled, and the rest were carried out of the PAPR by the airflow.

Figure 4 presents outward particle leakage at different particle sizes, breathing conditions, and supplied-air flowrates cumulated over all three breaths. The particle outward leakage indicates the percentage of exhaled particles leaking outside of the PAPR. The highest particle outward leakage, 75.50%, appeared in the CFD simulation of particle size 0.1 μm, light breathing, and a supplied-air flowrate 205 L/min, and the lowest one, 32.39%, appeared in the CFD simulation of particle size 10 μm, heavy breathing, and a supplied-air flowrate 100 L/min. The outward particle leakage increased as particle size decreased, breathing workload decreased, and the supplied-air flowrate increased.

Figure 5 presents the outward concentration leakage at different particle sizes, breathing conditions, and supplied-air flowrates. The outward concentration leakage indicates the comparison between the exhaled particle concentration leaking outside the PAPR and the exhaled particle concentration inside the PAPR. The highest outward leakage concentration, 49.29%, appeared in the CFD simulation of particle size 0.1μm, heavy breathing, and a supplied-air flowrate of 100 L/min, and the lowest one, 7.57%, appeared in the CFD simulation of particle size 10 μm, light breathing, and a supplied-air flow rate of 205 L/min. The outward concentration leakage increased as particle size decreased, breathing workload increased, and the supplied-air flowrate decreased.

To analyze the outward leakage of exhaled particles from PAPR wearers, we defined two parameters, the particle outward leakage and the concentration outward leakage (see Equation 5 and 6). The particle outward leakage evaluated the number of exhaled particles leaking outside of the PAPR, while the outward concentration leakage evaluated the concentration of exhaled particles leaking outside of the PAPR. The latter is more related to the experimental measurement in Kim and Hale [Kim et al, 2017], which measured the exhaled particle concentration outside PAPR. Because the PAPR system used in the CFD simulations has a loose-fitting face cover hood, unlike the hood style in the PAPR system used in Kim and Hale [Kim et al, 2017], exhaled particles were able to move outside of the PAPR through the gap at the loose-fitting faceseal.

Because the breathing air in the simulations was cyclic flow with both inhalation and exhalation, the real-time leakage of the exhaled particles was in unsteady-state. While this study simulated only three breaths for reducing the computational costs, larger number

of breaths may need to be simulated to reach steady-state. A future study will verify the influence of the number of breaths by choosing three different numbers (e.g., 60, 90, and 150 breaths) and conforming whether the leakage is converged.

The CFD simulation results show that the particle size, breathing conditions, and the supplied-air flowrates all have an impact on the outward leakage. Coarse particles (size ≥ 5 μm) are more likely to deposit inside PAPR than fine particles (size < 5 μm). Hence, the increase of particle size decreased both the outward particle leakage and the concentration outward leakage. A strong supplied-air flow pushes exhalation particles to leak out of PAPR and reduces the chance of particle depositing inside PAPR inlet covering, while it makes a big air volume to come out of PAPR and dilutes the exhalation particle concentration as the concentration equals the particle counts divided by air volume. Therefore, the increase of the supplied-air flowrate increased the particle outward leakage but decreased the outward concentration leakage. Although the heavy breathing airflow makes the particle more likely to deposit inside PAPR, it produces more exhaled particles, reducing the dilution level from the supplied-air flow. Consequently, the increase of the breathing workload decreased the outward particle leakage but increased the outward concentration leakage.

The primary limitation is that empiric particulate data is needed for understanding the entire spectrum of research questions about exhalation particles of PAPRs, as well as for validating the CFD results. This numerical study only considered mouth breathing, not cough or sneeze that the paper should identify as the major concern. Additionally, we ignored the particle dispersion from random motions of particles due to diffusion or turbulence [Tsuda et al, 2013]. Another limitation was that we assumed a linear relationship between breathing volume and particle emission. We assumed that inhaled particles would not re-exhaled into the PAPR breathing zone, but particles can be re-exhaled.

To obtain high validity of the prediction, future studies will increase the CFD model's fidelity by considering different respiratory particle expelling situations, such as nose/mouth breathing, cough, and sneeze, and through modeling particle dispersion during particle tracking. The CFD model's fidelity can also be improved by simulating different headforms to evaluate the impact of headform sizes on exhalation particles of PAPRs.

In addition to the simulation-based study, a series of experimental studies is also needed. First, the CFD simulation results will be validated by conducting experiments on a physical headform that will connect a breathing machine using the same breathing loads, supplied-air flow rates, and particle sizes as the ones defined in this study. Second, the design of the experiments for measuring the exhaled particles of PAPR via tuning experimental sceneries, including the particle probing location, the testing chamber's ventilation, and the particle counter's settings may be optimized. The computational work in this study can provide knowledge to the experimental optimization. Third, human subjects will be recruited to conduct tests using the optimized design of the experiments so that the results can be accepted by PAPR manufacturers and standard developers to make recommendations and decisions on whether PAPRs can be used in surgical settings.

CONCLUSIONS

The CFD simulations were capable of studying the mechanisms contributing to outward concentration leakage of exhaled particles by the loose-fitting PAPR wearers. The outward concentration leakage was low at surgical setting, e.g., it was about 9% for a particle size of 0.1 and 1 μm at light breathing and a 205 L/min supplied-air flowrate, which was similar to a healthcare worker's breathing workload in an OR. The supplied-air flow rates, particle sizes, and breathing workloads had effects on the outward concentration leakage, as the outward concentration leakage increased as particle size decreased, breathing workload increased, and the supplied-air flowrate decreased.

This study is an initial step toward better understanding the consequences of PAPR wearers exhaling viable infectious particles into a sterile surgical field. Empiric data drawn from well-designed clinical studies are urgently needed. The simulation results indicate that supplied-air flowrates, particle sizes, and breathing workloads are important factors about loose-fitting usage in surgical settings. The CFD simulations can help to optimize the supplied-air flowrates. When the loose-fitting PAPR is used, the exhaled particles with small size (below 1μm), or the heavy breathing workloads may generate a great risk to the sterile field and should be avoided. Furthermore, this study suggests that the breathing characteristics of wearers need to be monitored and evaluated in the development of future clinical studies on loose-fitting PAPRs.

Acknowledgements

The authors thank the following persons for their contributions: Lewis Radonovich, Ronald Shaffer, Harold Boyles, Debbie Novak, and Bill King.

REFERENCES

Da Zhou C, Sivathondan P, and Handa A, 2015, Unmasking the surgeons: the evidence base behind the use of facemasks in surgery. Journal of the Royal Society of Medicine, 108(6): p. 223–228. [PubMed: 26085560]

Lipp A and Edwards P, 2014, Disposable surgical face masks for preventing surgical wound infection in clean surgery. Cochrane Database of Systematic Reviews, (2).

CDC. Healthcare-associated Infections Data. 2018 Feb 4, 2019; Available from: https://www.cdc.gov/hai/data/index.html.

Skinner M and Sutton B, 2001, Do Anesthetists Need to Wear Surgical Masks in the Operating Theatre? A Literature Review with Evidence-Based Recommendations. Anesthesia and intensive care, 29(4): p. 331–338.

Wizner K, et al. , 2016, Prevalence of Respiratory Protective Devices in U.S. Health Care Facilities: Implications for Emergency Preparedness. Workplace Health & Safety, 64(8): p. 359–368. [PubMed: 27462029]

Sreeramoju PV and Cadena J, 2018, Airborne Precautions and Personal Protective Equipment: The Powered Air-Purifying Respirator-Only Approach, in Infection Prevention., Springer. p. 285–291.

Papineni RS and Rosenthal FS, 1997, The Size Distribution of Droplets in the Exhaled Breath of Healthy Human Subjects. Journal of Aerosol Medicine, 10(2): p. 105–116. [PubMed: 10168531]

Wurie F, et al. , 2013, Characteristics of exhaled particle production in healthy volunteers: possible implications for infectious disease transmission. F1000Research, 2: p. 14–14. [PubMed: 24555026]

Yan J, et al., 2018, Infectious virus in exhaled breath of symptomatic seasonal influenza cases from a college community, 115(5): p. 1081–1086.

Kim Y and Hale M, 2017, Pilot Study to Examine the Use of a Powered Air Purifying Respirator (PAPR) in the Operating Room, American Journal of Infection Control, 45(6): p. S84.

Grinshpun S, 2016, Simulation Study: Does the Air Exhaled from a PAPR Wearer Contaminate the Sterile Field in an Operating Room? Final Report.

Lei Z, Zhuang Z, and Bergman M, 2017, Application of digital human modeling for evaluating loose-fitting powered air-purifying respirators. in Proceedings of the 5th international digital human modeling symposium.

Bergman M, Lei Z, Xu S et al., 2018, Validation of Computational Fluid Dynamics Models for Evaluating Loose-Fitting Powered Air-Purifying Respirators. in Congress of the International Ergonomics Association, IEA 2018, AISC 819, pp. 176–185, Springer Nature Switzerland.

Benson S and Viscusi D, 2010, Digital 3-D headforms with facial features representative of the current US workforce AU - Zhuang, Ziqing, Ergonomics, 53(5): p. 661–671. [PubMed: 20432086]

Adams WC, 1993, Measurement of breathing rate and volume in routinely performed daily activities: final report, contract no. A033–205.

Anderson NJ, et al. , 2006, Peak inspiratory flows of adults exercising at light, moderate and heavy work loads. Journal-international society for respiratory protection, 23(1/2): p. 53.

Lindsley WG, et al. , 2012, Dispersion and exposure to a cough-generated aerosol in a simulated medical examination room, Journal of occupational and environmental hygiene, 9(12): p. 681690.

Tsuda A, Henry FS, and Butler JP, 2013, Particle transport and deposition: basic physics of particle kinetics. Comprehensive Physiology, 3(4): p. 1437–1471. [PubMed: 24265235]

Figure 1.
MaxAir® 78SP-36 cuff system (Photos Credit: NIOSH/NPPTL).

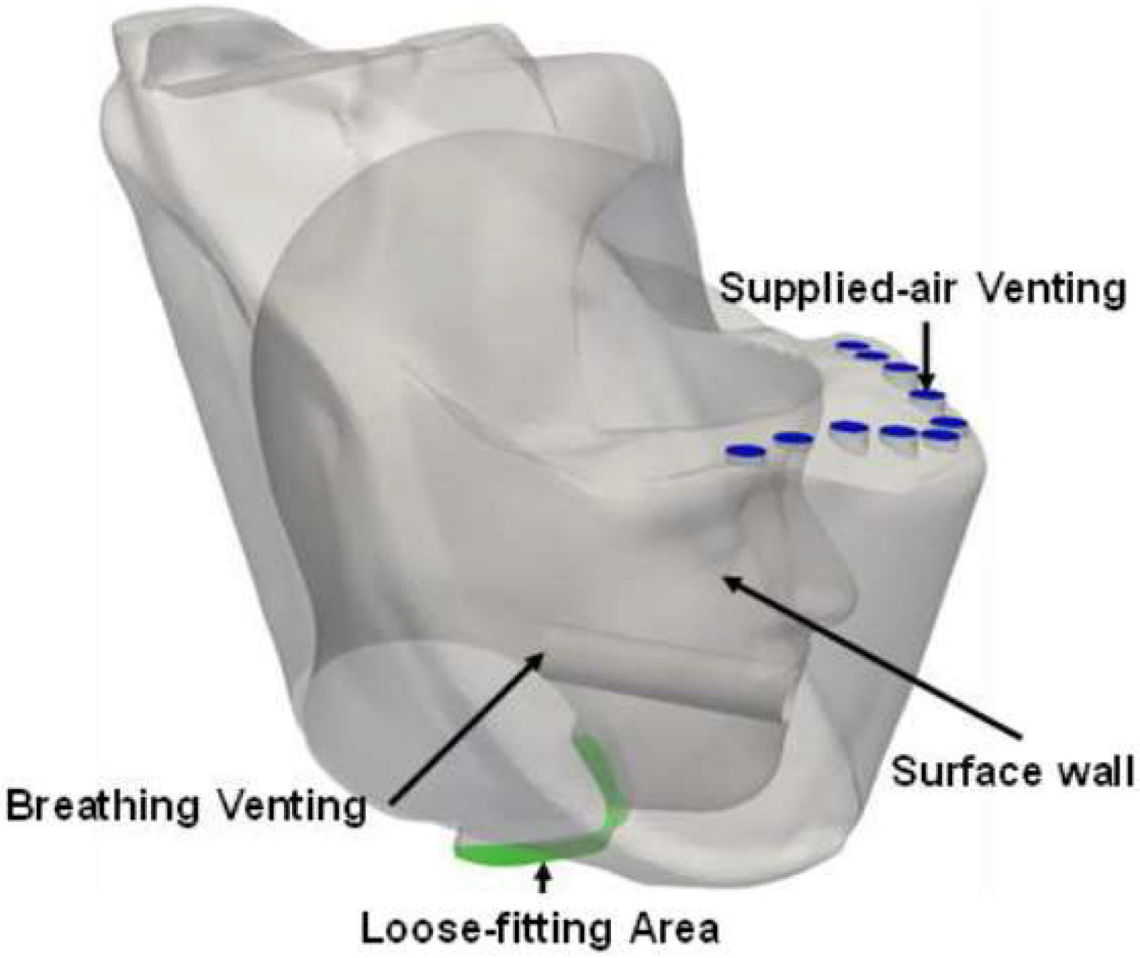

Figure 2.
CFD model of PAPR-headform.

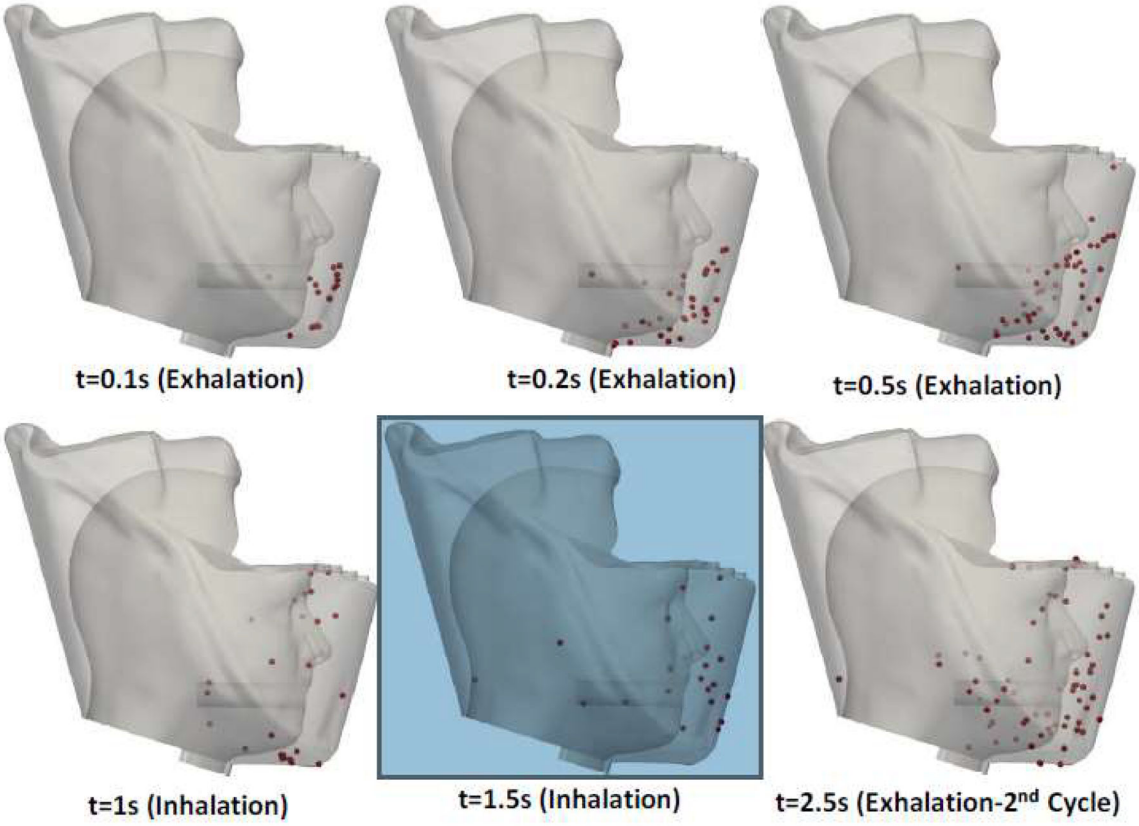

Figure 3:
Particle distribution inside the PAPR inlet covering at different time instances of a breathing cycle (heavy workload, supplied-air flow rate 205 L/min, and particle size 1 μm).

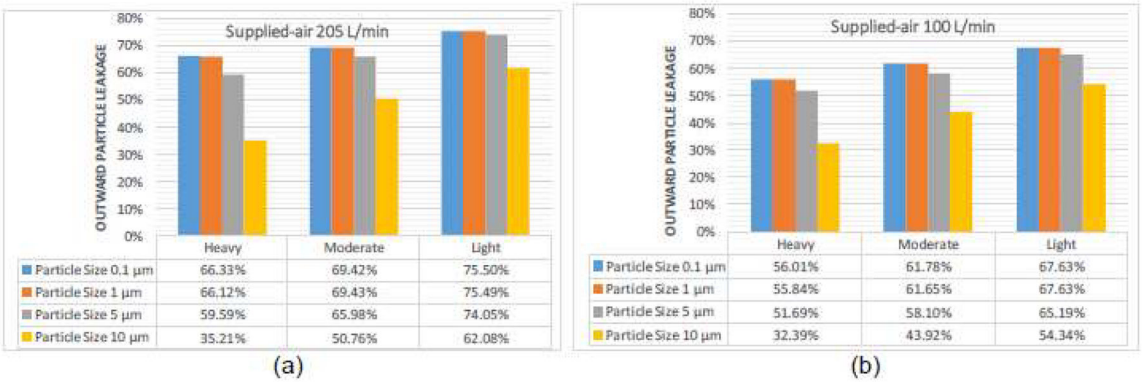

Figure 4:

Particle outward leakage of different particle sizes, breathing conditions, and supplied-air flow rates; (a) supplied-air flow rate 205 L/min, and (b) supplied-air flowrate 100 L/min.

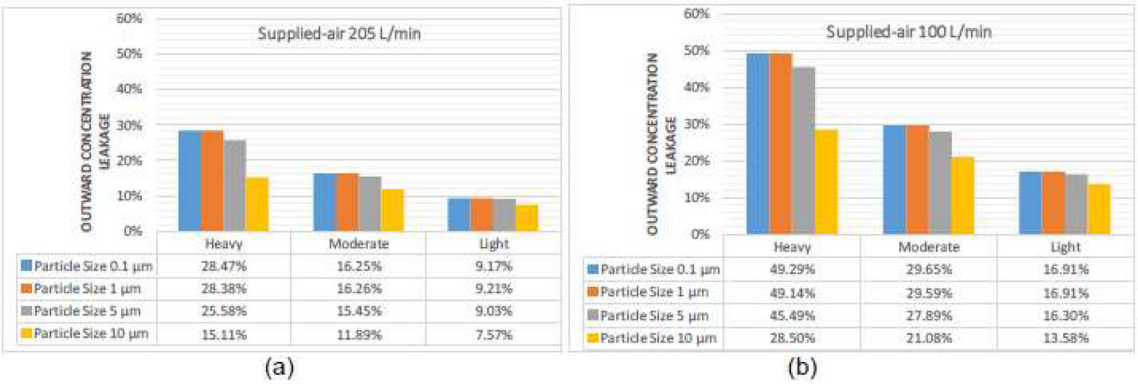

Figure 5:

Concentration outward leakage of different particle sizes, breathing conditions, and supplied-air flowrates; (a) supplied-air flowrate 205 L/min, and (b) supplied-air flowrate 100 L/min.

Table I.

Representative Task Activities with Associated Work Rate and Minute Ventilation [Anderson et al, 2006]

Task activity	Work rate	Minute ventilation YE (L/min)	Frequency (Breaths/ min)
Light work (standing or working in an operating room and carrying weight <25 lbs)	Light	25	20
Moderate exertion (lifting or moving patients i.e., weight > 100 lbs)	Moderate	48	27
Heavy work (Emergency situation)	Heavy	88	32